Supporting Information

First-principles Study on the Catalytic Performance of Transition Metal Atom doped $CrSe_2$ for Oxygen Reduction Reaction

Long Lin[a,b], Yadan Sun[a], Kun Xie[a], Pei Shi[a], Xinyu Yang[a], Dongbin Wang[*c]

[a] *Cultivating Base for Key Laboratory of Environment-Friendly Inorganic Materials in Henan Province, School of Materials Science and Engineering, Henan Polytechnic University, Jiaozuo 454000, China*

[b] *School of Mathematics and Informatics, Henan Polytechnic University, Jiaozuo 454000, China*

[*c] *School of Materials Science and Engineering, Henan Polytechnic University, Jiaozuo 454000, China. Email: wdbyxr@163.com*

Corresponding author: *wdbyxr@163.com*

Table S1. The parameters of the adsorption energy (E_{ads}), adsorption height and the difference of the distance of O-O (Δd) of O_2 after its adsorption on the surface of intrinsic $CrSe_2$, where site I, II, III, IV represents the top site of Cr, the top of Se from the top layer, the bridge site of Cr-Se, the top of Se from the bottom layer, respectively.

Configuration		E_{ads} (eV)	Height (Å)	Δd (Å)
Orientation	Site			
End-on	I	0.483	2.859	0.019
	II	0.046	2.491	0.020
	III	-0.122	2.647	0.011
	IV	-0.112	2.498	0.013
Side-on	I	-0.494	3.019	0.006
	II	-0.133	2.758	0.014
	III	-0.110	2.788	0.013
	IV	-0.100	2.683	0.014

Table S2. The formation energy (E_f) of different TM atom.

Doped TM	E_f (eV)
Rh	-1.098
Pd	-0.372
Ag	0.650
Ir	-2.196
Pt	-1.867
Au	-0.201

Table S3. The adsorption energy (E_{ads}) of O_2 on different sites of TM-doped $CrSe_2$ systems, the distance between O-O ($d_{O\text{-}O}$), and the Bader charge transfer (ΔQ).

System	Configuration		E_{ads} (eV)	$d_{O\text{-}O}$ (Å)	ΔQ (e)		
	Orientation	Site			TM	O_2	Substrate
Rh-$CrSe_2$	Side-on	B	-1.505	1.292	-0.142	0.399	-0.256
		T	-2.008	1.399	-0.292	0.645	-0.353
	End-on	B	-1.394	1.296	-0.129	0.353	-0.223
		T	-1.661	1.294	-0.138	0.405	-0.267
Pd-$CrSe_2$	Side-on	B	-0.422	1.275	-0.041	0.207	-0.166
		T	-0.336	1.266	-0.061	0.227	-0.166
	End-on	B	-0.431	1.285	-0.043	0.314	-0.271
		T	-0.117	1.259	-0.017	0.216	-0.199
Ir-$CrSe_2$	Side-on	B	-1.249	1.300	-0.020	0.439	-0.418
		T	-1.754	1.449	-0.239	0.706	-0.467
	End-on	B	-1.203	1.303	0.027	0.408	-0.435
		T	-1.246	1.301	-0.017	0.443	-0.426
Pt-$CrSe_2$	Side-on	B	-0.692	1.295	0.144	0.368	-0.513
		T	-0.198	1.294	0.139	0.363	-0.502
	End-on	B	0.385	1.238	0.461	0.120	-0.580
		T	-0.140	1.294	0.139	0.359	-0.498

Table S4. ΔG of intermediates adsorption and the four reaction steps, as well as the overpotentials (η) of ORR on TM-doped $CrSe_2$.

System	ΔG_{OOH*} (eV)	ΔG_{O*} (eV)	ΔG_{OH*} (eV)	ΔG_1 (eV)	ΔG_2 (eV)	ΔG_3 (eV)	ΔG_4 (eV)	η^{ORR} (V)
Rh_{S_T}-$CrSe_2$	2.483	0.445	-0.562	-2.437	-2.038	-1.007	0.562	1.79
Ir_{S_T}-$CrSe_2$	3.120	0.256	-0.134	-1.800	-2.864	-0.390	0.134	1.36
Pt_{S_B}-$CrSe_2$	4.006	1.666	0.937	-0.914	-2.340	-0.729	-0.937	0.50
Pd_{E_B}-$CrSe_2$	3.808	2.617	0.799	-1.112	-1.190	-1.819	-0.799	0.43

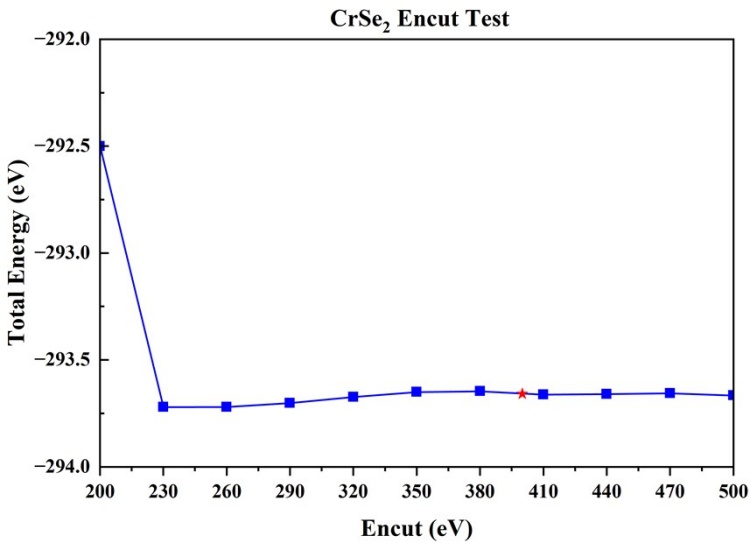

Fig. S1. The cutoff energy test results from 200 to 500 eV, with an interval of 30 eV.

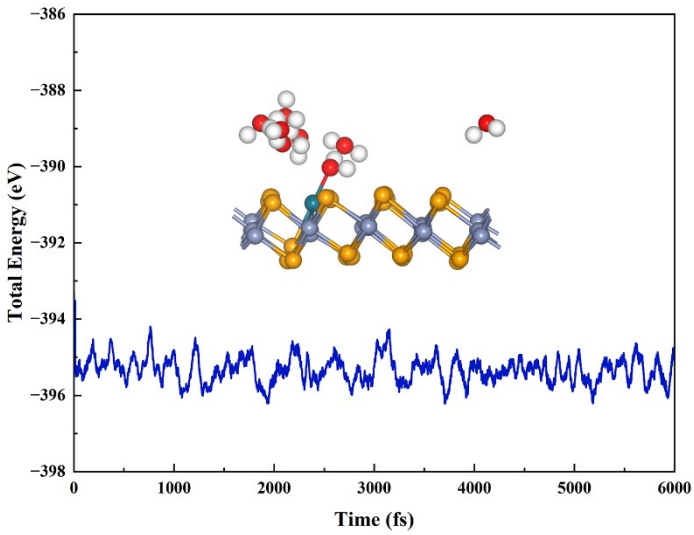

Fig. S2. The total energy variation and the configuration of Pd-$CrSe_2$ at 300 K under AIMD simulation.

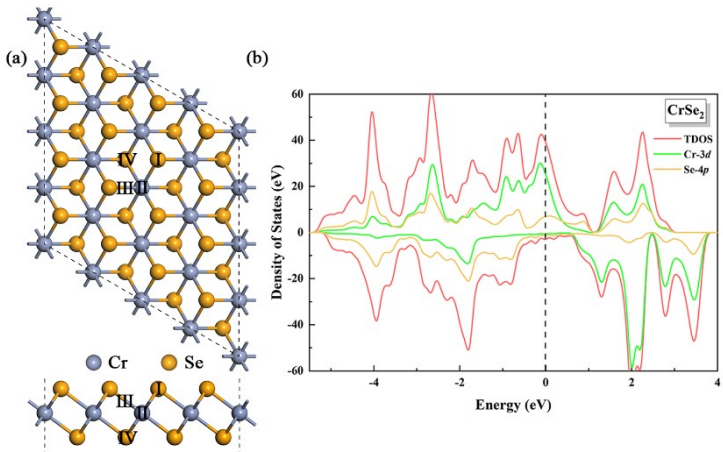

Fig. S3. The optimized structure, the adsorption sites, and the density of states (DOS) of the intrinsic $CrSe_2$.

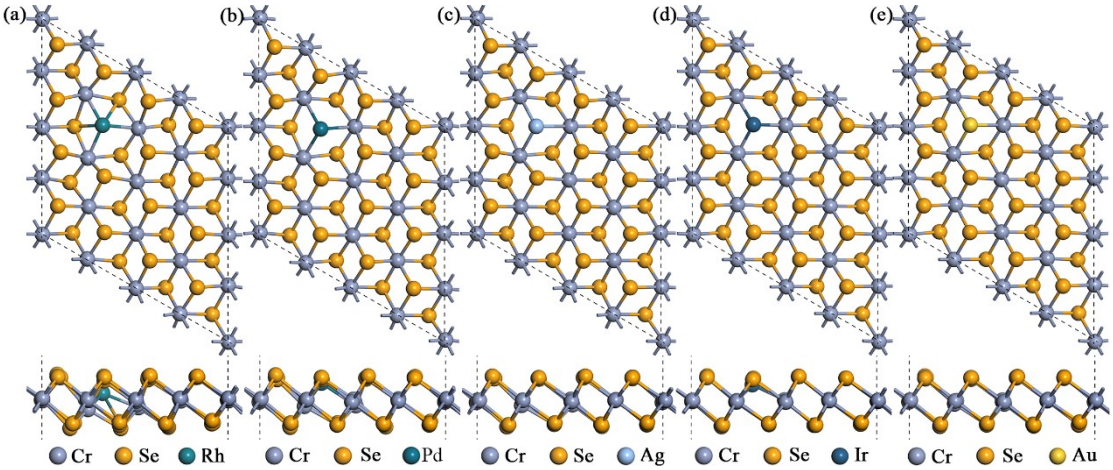

Fig. S4. (a)-(e) The optimized structure of Rh-$CrSe_2$, Pd-$CrSe_2$, Ag-$CrSe_2$, Ir-$CrSe_2$, Au-$CrSe_2$, respectively.

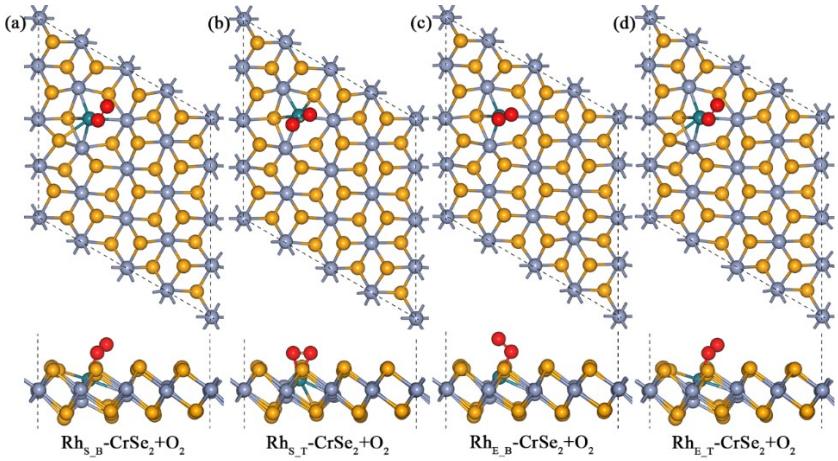

Fig. S5. Top and side views of O_2 adsorbed on the different sites of Rh-$CrSe_2$, (a) S_B (b) S_T, (c) E_B, (d) E_T, respectively.

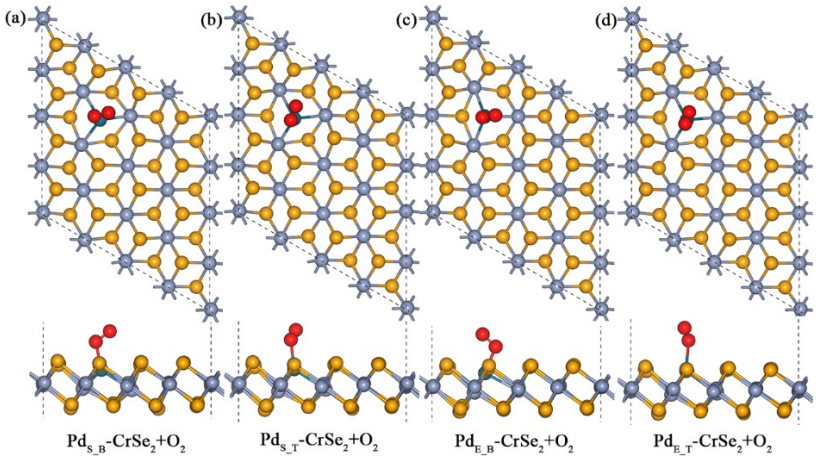

Fig. S6. Top and side views of O_2 adsorbed on the different sites of Pd-$CrSe_2$, (a) S_B (b) S_T, (c) E_B, (d) E_T, respectively.

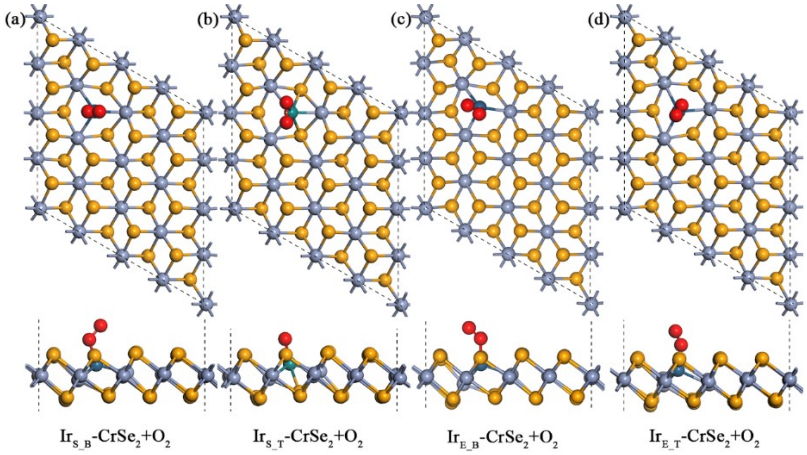

Fig. S7. Top and side views of O_2 adsorbed on the different sites of Ir-$CrSe_2$, (a) S_B (b) S_T, (c) E_B, (d) E_T, respectively.

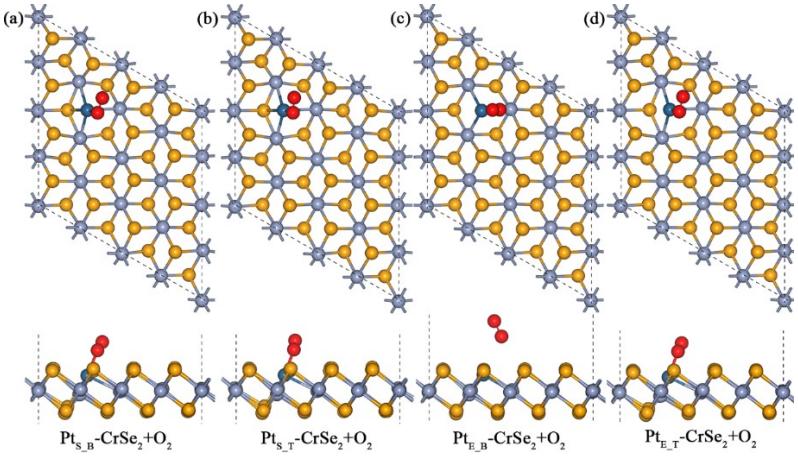

Fig. S8. Top and side views of O_2 adsorbed on the different sites of Pt-$CrSe_2$, (a) S_B (b) S_T, (c) E_B, (d) E_T, respectively.

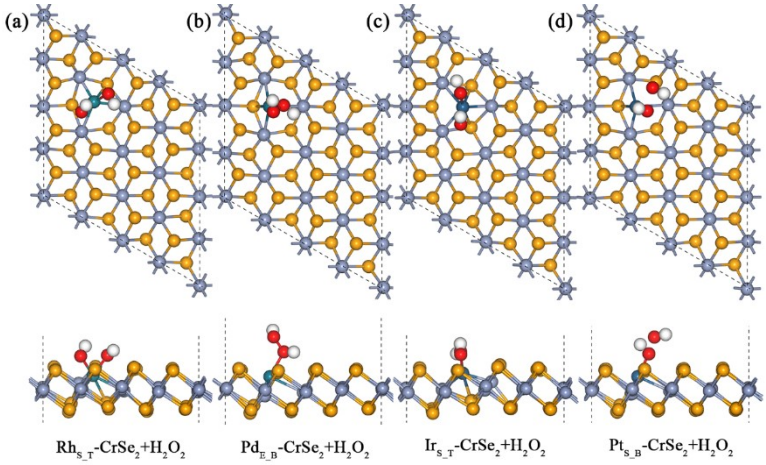

Fig. S9. The optimized structures of H_2O_2 adsorbed on the surface of (a) Rh_{S_T}-$CrSe_2$, (b)Pd_{E_B}-$CrSe_2$, (c) Ir_{S_T}-$CrSe_2$, (d) Pt_{S_B}-$CrSe_2$, respectively.

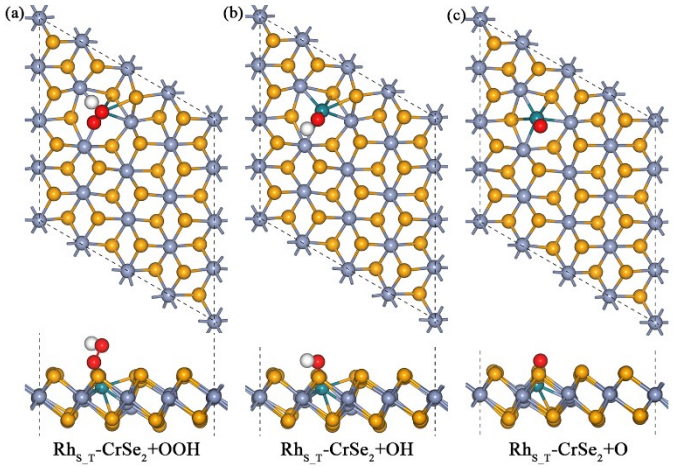

Fig. S10. The ORR intermediates adsorbed on Rh_{S_T}-$CrSe_2$.

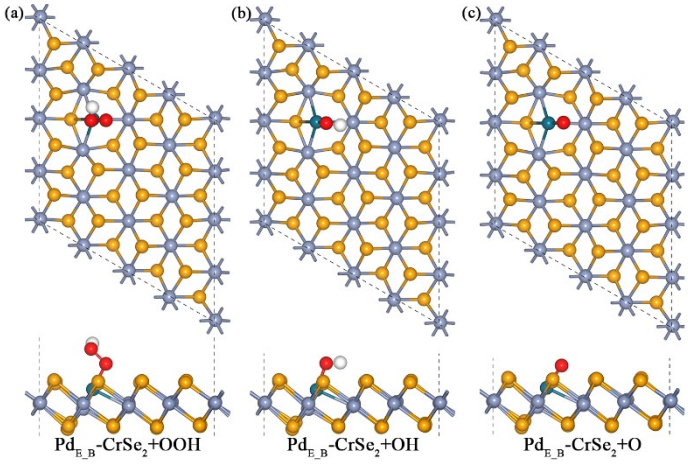

Fig. S11. The ORR intermediates adsorbed on Pd_{E_B}-$CrSe_2$.

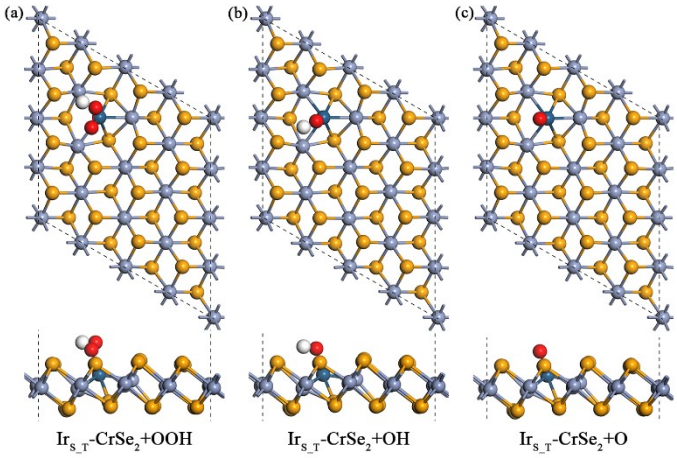

Fig. S12. The ORR intermediates adsorbed on Ir_{S_T}-$CrSe_2$.